International Journal of Nanomedicine

Dovepress
open access to scientific and medical research

Open Access Full Text Article

ORIGINAL RESEARCH

Icariin-loaded electrospun PCL/gelatin sub-microfiber mat for preventing epidural adhesions after laminectomy

This article was published in the following Dove Press journal:
International Journal of Nanomedicine

Yuelong Huang[1]
Rui Shi[2]
Min Gong[3]
Jingshuang Zhang[2]
Weiyang Li[2]
Qingpeng Song[1]
Chengai Wu[2]
Wei Tian[1]

[1]Department of Spine Surgery of Beijing Jishuitan Hospital, The Fourth Clinical Medical College of Peking University, Beijing 100035, China; [2]Institute of Traumatology and Orthopaedics, Beijing Laboratory of Biomedical Materials, Beijing Jishuitan Hospital, Beijing 100035, China; [3]Beijing Laboratory of Biomedical Materials, State Key Laboratory of Organic–Inorganic Composites, Beijing University of Chemical Technology, Beijing 100029, China

Background: Epidural adhesion is one of the major reasons attributed to failed back surgery syndrome after a successful laminectomy, and results in serious clinical complications which require management from physicians. Therefore, there is an urgent demand within the field to develop biodegradable anti-adhesion membranes for the prevention of post-operative adhesion.

Methods: In this study, icariin (ICA) was initially loaded into polycaprolactone (PCL)/gelatin fibers via electrospinning to fabricate nanofibrous membranes. The effects of the ICA content (0.5wt%, 2wt% and 5wt%) and the bioactivity of ICA in the nanofibrous membranes were investigated in vitro and in vivo.

Results: The nanofibrous membranes showed suitable pore size and good properties that were unaffected by ICA concentration. Moreover, the ICA-loaded membranes exhibited an originally rapid and subsequently gradual sustained ICA release profile that could significantly prevent fibroblast adhesion and proliferation. In vivo studies with rabbit laminectomy models demonstrated that the ICA-loaded membranes effectively reduced epidural adhesion by gross observation, histology, and biochemical evaluation. The anti-adhesion mechanism of ICA was found to be via suppression of the TGF-β/Smad signaling proteins and down regulation of collage I/III and a-SMA expression for the first time.

Conclusion: We believe that these ICA-loaded PCL/gelatin electrospun membranes provide a novel and promising strategy to resist adhesion formation following laminectomy in a clinical application.

Keywords: icariin, polycaprolactone/gelatin, electrospun, epidural adhesion

Introduction

Laminectomy is the classical surgical procedure for posterior spinal operation and is commonly used to provide effective nerve decompression. Although the treatment is effective, it does have several complications, with the main complications being adhesion and scar tissue formation. These processes are inevitable following laminectomy; however, they can lead to serious complications that are nominally referred to as failed back surgery syndrome.[1,2] Adhesions and fibrous scars extrude to the spinal dural causing nerve root compression, which results in radicular pain and functional impairment in the lower limbs. The pathophysiology mechanism of postoperative epidural fibrosis is not well understood, but the accepted view is that hematoma formation, the accumulation of inflammatory cytokines, fibroblast proliferation and collagen synthesis accelerate fibrous adhesion formation in the epidural operational area after surgical trauma.[3] Presently, the choice of precaution or mitigation strategy to minimize epidural adhesion remains a challenge. Therefore, studies to effectively

Correspondence: Rui Shi
Institute of Traumatology and Orthopaedics, Beijing Laboratory of Biomedical Materials, Beijing Jishuitan Hospital, No 31, Xinjiekou East Street, Xicheng District, Beijing 100035, China
Tel +86 105 851 7081
Fax +86 5 851 6538
Email sharell@126.com

Wei Tian
Department of Spine Surgery of Beijing Jishuitan Hospital, The Fourth Clinical Medical College of Peking University, No 31, Xinjiekou East Street, Xicheng District, Beijing 100035, China
Tel +86 105 851 7077
Fax +86 5 851 7077
Email tianwei123vip@163.com

submit your manuscript | www.dovepress.com
Dovepress
http://dx.doi.org/10.2147/IJN.S169427

prevent epidural fibrous processes and reduce scar formation are imperative post-laminectomy.

Icariin (ICA), a flavonoid glycoside, is extracted from the Chinese medicine *Herba Epimedii* and has been shown to be a relatively safe and non-toxic treatment. Much attention has been paid to the efficient roles of ICA in bone formation and cardiovascular disorders as well as its anti-tumor and anti-oxidant properties.[4] Additionally, ICA has been reported to inhibit collagen and fibronectin accumulation through downregulating the TGF-β protein in renal mesangial cells and regulating inflammatory response via TNF-α/IFN-γ signals.[5,6] Moreover, the anti-angiogenic activity of ICA was confirmed by the inhibition of the proliferation of vascular smooth muscle cells through inactivation of the ERK1/2 signaling pathway.[7] However, we are not aware of any studies focused on the anti-adhesion roles and mechanisms of ICA in blocking epidural adhesion formation.

Effective drug delivery systems are required to meet the needs of maintaining biological activity and biocompatibility. Electrospinning has currently gained widespread interest and can provide great flexibility for drug delivery applications.[8] This technique is capable of fabricating electrospun polymer microfibers with the required diameters and three-dimensional biological structures with high porosity, good permeability and sub-micrometer pore size.[8] Due to these properties, electrospun membranes are expected to offer a novel, biocompatible barrier to stop fibroblast penetration,[9] while providing high encapsulation efficiency to maintain a stable drug release profile.[10,11] Additionally, electrospun membranes possess the peculiarity of adjustable drug release rates and degradation rates, which can be controlled through judicious choice of the membrane parameters.[12] Therefore, we chose electrospinning as a reliable and versatile method to fabricate the requisite anti-adhesion membranes preloaded with specific therapeutic compounds.

Polycaprolactone (PCL) is a well-known non-cytotoxic, biocompatible and biodegradable polymer that exhibits strong flexibility and high mechanical strength and is deemed suitable for biomedical applications. PCL microfibrous membranes have been employed as anti-adhesion barriers in tendon healing and have successfully demonstrated their enhanced efficacy in preventing tendon adhesions.[13] However, PCL microfibers in anti-adhesion products have certain limitations due to an extremely long degradation period and high hydrophobicity, which is not ideal as a micropolymer biomaterial.[14] The hydrophobic nature of the polymers leads to a lack of cell adhesion sites, while low biodegradation rates have the potential to disturb self-repair ability in vivo. To overcome these fundamental drawbacks, blending PCL with natural polymer such as gelatin may provide superior microfibers that exhibit improved biodegradation rates and hydrophilicity. Gelatin, derived from hydrolysis of natural occurring collagen, is a widely utilized biopolymer with low immunogenicity, fast degradation rates and a highly hydrophilic surface.[15] This PCL/gelatin hybrid nanofiber, a novel biomaterial with tunable properties, has been successfully used in various drug delivery systems and tissue regeneration applications.[15–17] Additionally, these two polymers are commercially available at low cost and are easily obtained, and hence, they have tremendous potential in various biomedical fields.

Therefore, the purpose of this study is to apply a novel and efficient electrospinning technique to fabricate ICA-loaded PCL/gelatin microfiber membranes for the prevention of scar tissue and adhesion formation in post-laminectomy patients. We investigated the effects of ICA content on the surface morphology, drug release profiles and in vitro/in vivo biological properties. To understand the anti-adhesive mechanism of ICA, epidural adhesion tissues were used to determine collagen and TGF-β/Smad protein expression (Scheme 1).

Materials and methods

Materials

PCL (Mw =70 kDa; purity: 99%), Cell Counting Kit-8 (CCK-8), hydroxyproline kit and MTT were purchased from Sigma-Aldrich Co. (St Louis, MO, USA). Gelatin (purity: 99.5%) was purchased from Rousselot (Rambouillet, France). ICA (purity>97%) and acetic acid (purity: 99.8%) were supplied by Sinopharm Chemical Reagent Beijing Co. Ltd. (Beijing, China). DMEM, fetal bovine serum (FBS), penicillin–streptomycin and PBS were obtained from Thermo Fisher Scientific (Waltham, MA, USA). Trifluoroethanol (TFE) was purchased from Alfa-Aesar Chemical Inc. (MA, USA). Polyformaldehyde, Triton X-100, DAPI and fluorescein isothiocyanate (FITC)–phalloidin were purchased from Beyotime Institute of Biotechnology (Shanghai, China).

Electrospinning of microfiber membranes

The electrospun PCL–gelatin (blended with the mass ratio of 4:1) solution was prepared by dissolving each polymer in TFE with an overall concentration of 8 wt%. To avoid phase separation between PCL and gelatin, a small quantity of acetic acid (0.2 v/v% TFE) was added to the mixed liquid to acquire a homogeneous and hyaline PCL–gelatin solution. For loading the ICA by electrospinning, the ICA powder was directly dissolved in the PCL–gelatin solution with various

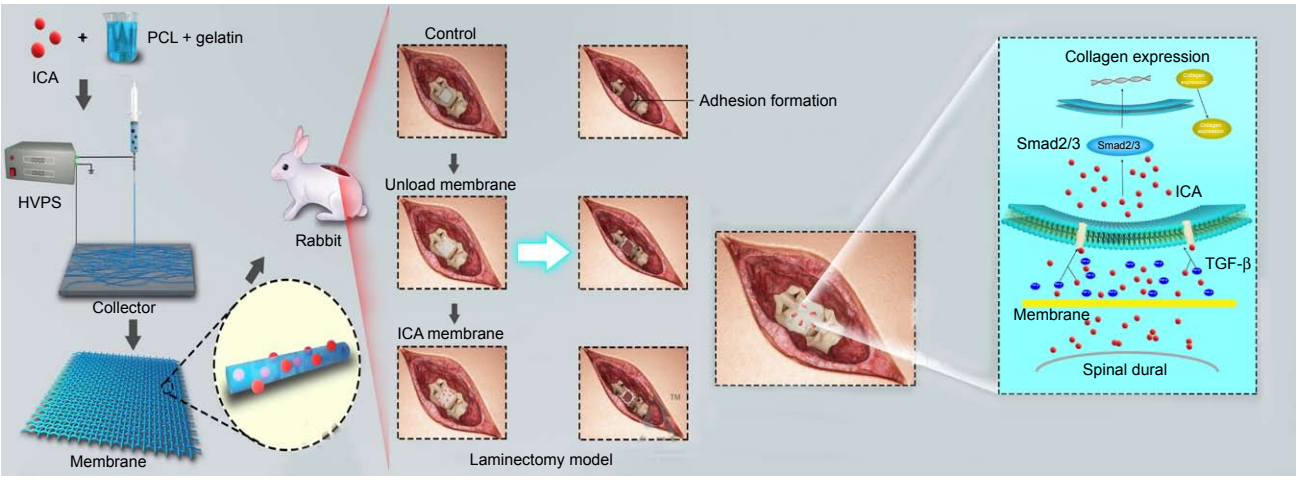

Scheme 1 Schematic illustration of preparing PCL–gelatin membrane and the use of PCL–gelatin membrane in the laminectomy model to prevent adhesion formation, and the diagram showing the possible ways of inhibition of the TGF-β and Smad pathways by ICA.
Abbreviations: HVPS, high-voltage power supply; ICA, icariin; PCL, polycaprolactone.

concentrations (unloaded control, 0.5 wt%, 2 wt% and 5 wt%). A syringe pump was used to feed the PCL–gelatin solution into the needle tip at a flow rate of 1.5 mL/h. An optimized voltage of 12–18 kV and a suitable distance of 20 cm were applied between the needle and the grounded collector that was rotating at the rate of 300 rpm. The microfibrous membranes were collected on a grounded collector with aluminum foil. The fabricated microfiber membranes were dried overnight at room temperature under vacuum before use.

Morphology, chemical structure and mechanical property characterizations

The morphology of PCL–gelatin microfiber membranes was observed by scanning electron microscopy (SEM) and is recorded at 5 kV sputtering energy. The average fiber diameter and pore size were analyzed by measuring at least 100 random sites with the Image J software from the SEM images.

Fourier transform infrared spectra (FTIR) were used to evaluate the chemical–structural properties of the membranes with a Bruker Tensor 27 spectrometer. The spectra wavelength ranges from 4,000 cm^{-1} to 600 cm^{-1} with the resolution of 2 cm^{-1}. Differential scanning calorimetry (DSC) was used to determine the thermal properties of the microfiber membranes. The membranes were placed in an aluminum crucible, and the analysis was performed from −100°C to 220°C at a cooling and heating rate of 10°C min^{-1} under a nitrogen atmosphere.

To detect the mechanical properties, the electrospun membranes were cut into small strips with dimensions of 25×4×1 mm. The tensile property was evaluated by using a BOSE ElectroForce 3200 instrument with a 50 n load at a stretching speed of 5 mm/min, which ultimately transforms into the stress–strain curves.

The static water contact angle (WCA) of electrospun membrane was measured using a SL200A type Contact Angle Analyzer (Solon Technology Science Co., Ltd., Shanghai, China). Water droplets (2.0 µL) were dropped onto the surface of the membrane. The average WCA value was obtained by measuring six water droplets at randomly distributed positions.

In vitro drug release profiles

PBS (pH 7.4) was used to imitate a typical physiological environment. The electrospun membranes were cut into specimens of 2 cm in diameter (total mass =60 mg) and then incubated in 10 mL of PBS at 37°C with slight shaking. At each time interval, 10 mL of released supernatant was collected and replaced with fresh PBS of equal volume. The quantity of released ICA in the supernatant was measured by ultraviolet visible spectrophotometry (UV-2550; Shimadzu, Kyoto, Japan) at 290 nm; meanwhile the percentage of released drug was calculated according to the initial ICA weight in the electrospun membranes.

In vitro cell studies

L929 fibroblast cell lines were kindly donated by Institute of Beijing Traumatology and Orthopedics. All the procedures of cell studies were approved by the ethics institutional review committee of Beijing Jishuitan Hospital.

Barrier function to fibroblast cells

The in vitro barrier function of the blending electrospun membranes was evaluated using L929 cells as a cellular model. The electrospun membranes of different groups were cut into circular disks (diameter, 25 mm) and then fixed in a Cell Crown™ (Sigma-Aldrich Co.). The fixed membranes were sterilized by immersing in 75% ethanol for 1 hour, rinsed three times with PBS and placed into a 24-well culture plate. A suspension of L929 cells in culture medium containing DMEM, 10% (v/v) FBS and 1% penicillin–streptomycin was seeded onto the membrane surfaces at a density of 3.0×10^4 cells/mL. After incubating at 37°C under a 5% CO_2 atmosphere for 1 day, 4 days and 7 days, the fixed membranes were drawn out to observe the penetration results in the reverse side of membranes and the bottom of the culture plates by SEM and inverted phase contrast microscopy (Olympus IX50-S8F2), respectively.

Cell attachment observation studies

L929 cells were seeded onto various electrospun membranes in a 24-well plate at a density of 2.0×10^4 cells/cm^2. After incubating for 4 days, the cell attachments on the fibrous membranes were evaluated by actin and nuclear staining for fluorescent observation. First, membranes with cells were washed in PBS for three times, fixed in 4% paraformaldehyde for 20 minutes and then permeabilized with 0.1% Triton X-100 for 10 minutes at room temperature. Second, the cell-cultured membranes were stained with FITC–phalloidin solution (5 mg/mL) for 30 minutes and then with DAPI (1 mg/mL) for 5 minutes. After washing with PBS, the cell morphologies on the surface of the membranes were observed under the fluorescence microscope (LEICA DM 4000 B, Wetzlar, Germany). Nuclei were stained bright blue, and actin cytoskeleton was stained green.

Cell cytotoxicity and proliferation assay

The membrane samples (20×20 mm) were sterilized by immersing in 75% (v/v) ethanol and exposed to an ultraviolet lamp for 30 minutes, followed by incubation in culture medium (2 cm^2/mL) for 48 hours to obtain the extract solution. The filtered extract solution was regarded as a special culture medium to resuspend the L929 cells at a density of 2.0×10^4 cells/mL in 96-well micrometer plates, and the ordinary culture medium as a blank control and DMSO solution as a negative control. After incubating at 37°C under a 5% CO_2 humidified atmosphere for 1 day, 4 days and 7 days, an MTT assay and acridine orange–ethidium bromide (AO-EB) kit were used to determine the cytotoxicity in the extract solution. After double staining with the AO-EB kit, the cell morphology and dead/live cells were observed using the fluorescence microscope (Olympus IX50-S8F2). Additionally, the cells treated with MTT (5 mg/mL) were cultured for another 4 hours in the same atmosphere, and then the MTT was replaced with the same volume of DMSO to dissolve the formazan crystals. The OD was then detected on a microplate reader at 570 nm.

The relative growth rate (RGR/%) represents the cell viability in the extract solution and was calculated on the basis of the equation:

$$\mathrm{RGR}\% = \frac{\mathrm{OD\ (extract)} - \mathrm{OD\ (negative)}}{\mathrm{OD\ (blank)} - \mathrm{OD\ (negative)}}.$$

Based on the standard of GB/T16175-2008, the RGR was divided into six grades: Grade 0, RGR/% =100; Grade 1, RGR/% =75–99; Grade 2, RGR/% =50–74; Grade 3, RGR/% =25–49; Grade 4, RGR/% =1–24 and Grade 5, RGR/% =0. Grades 0–2 were considered as eligible, whereas Grades 3–5 were treated as unqualified.

The proliferation of L929 cells on the membranes was assessed by using a CCK-8 assay. The circular membranes fixed in a Cell Crown were sterilized and put into 24-well plates. Cell resuspensions were added into the wells on the fixed membranes at a density of 3.0×10^4 cells/mL. After 1 day, 4 days and 7 days of incubation, diluent CCK-8 solution was added onto the membranes to detect the live cells. After culturing for 2 hours, 200 μL of supernatants was transferred into a 96-well plate to measure the OD at 450 nm, which was calculated according to the standard curve of CCK-8 specification.

In vivo anti-adhesion study

All procedures of the animal study were approved by the ethics institutional review committee of Beijing Jishuitan Hospital. The welfare of the animals was in accordance with the "Laboratory Animals-Guideline of welfare and ethics" of the State Standard of the People's Republic of China. Thirty-six male New Zealand White rabbits, 6 months old and weighing 2.0–2.5 kg, were used in this study.

Laminectomy model

Rabbits were anesthetized by intramuscular injections of ketamine (0.4 mL/kg). The longitudinal midline incision was made in the skin, and the subcutaneous fascia and muscles were separated to expose the fifth lumbar vertebral lamina. Rongeur forceps were used to remove the spinous process, vertebral lamina and ligamentum flavum to create a 3×5 mm lamina defect, so that the spinal dural and spinal

cord were visible. The animals were then randomly divided into five groups, including a blank control group, an unloaded control group and three experimental groups (0.5%, 2% and 5% ICA). In the unloaded group and three experimental groups, 4×6 mm pieces of electrospun fibrous membranes were laid onto the lamina defects, and the incisions were closed with sutures (Figure 1).

Adhesion scores and hydroxyproline analysis

After 4 weeks post-surgery, the adhesion tissues were harvested from the posterior of spinal dural and graded according to the Rydell standard (Grade 0: no adhesion to dura mater; Grade 1: adhesion to dura mater, but easily dissected; Grade 2: adhesion to dura mater, and difficultly dissected; and Grade 3: firm adhesion to dura mater, and could not be dissected).[18] The samples were then analyzed by using a hydroxyproline testing kit. The adhesion tissues were adequately hydrolyzed in extracting solution, and the supernatant blending with color reagents was then drawn to detect the absorbance at 560 nm by using a spectrometry photometer (UV-2550; Shimadzu). According to the standard curve, the contents of hydroxyproline in various tissues were calculated, respectively, by the absorbance value.

Histological evaluation and membrane biodegradation observations

After 4 weeks, the rabbits were sacrificed, and the lumbar vertebras were separated to fix in 4% paraformaldehyde for 7 days, and then decalcified in 30% formic acid for 2 weeks. The specimens were sectioned into 4 μm slices and stained with H&E and Masson trichrome following the standard protocols. The adhesion formation and inflammatory reaction in different groups were observed under a stereoscopic microscope. Explanted membranes were observed by macroscopic evaluation and SEM at different periods (1 month, 2 months and 3 months).

Western blot analysis

Adhesion tissues behind the spinal dural in different groups were collected and homogenized in 300 mL RIPA (Bio-Rad Laboratories Inc., Hercules, CA, USA). The mixed lysates were stewing on ice for 30 minutes and centrifuged at 12,000 rpm in a refrigerated centrifuge for 15 minutes to extract the supernatant. The protein concentrations of the supernatant were determined by a BCA protein assay kit (Thermo Fisher Scientific). The samples were electrophoresed through 10% sodium dodecyl sulfate polyacrylamide gel electrophoresis (SDS-PAGE) gel and transferred onto polyvinylidene fluoride (PVDF) membranes. Afterward, the membranes were incubated with antibodies (diluted 1:1,000, Abcam, Cambridge, MA, USA) against β-actin, collagen I (col I), collagen III (col III), α-SMA and TGF-β/SMAD2/3 at 4°C overnight, followed by incubation with the secondary antibodies (diluted 1:2,000; ZSGB-BIO, Beijing, China) at 37°C for 1 hour. Finally, the membranes were washed with TBST buffer for three times, and the protein bands were scanned with an imaging system (Image Quant LAS 4000 mini, GE Healthcare Bio-Sciences AB, Uppsala, Sweden).

Statistical analyses

All statistical analyses were performed using SPSS version 19.0 (IBM Corporation, Armonk, NY, USA), and the results were expressed as mean±SD. ANOVA was conducted to compare trends among different groups, with the level of significance set at $P<0.05$.

Results

Characterization of PCL–gelatin electrospun membranes

The morphology of the electrospun membranes

As shown in the SEM micrographs (Figure 2A and B), ICA-loaded PCL–gelatin electrospun membranes were successfully fabricated with randomly interconnected structures with

Figure 1 The laminectomy process in rabbit models.
Note: (**A**) The arrow indicates spinous process, vertebral lamina, (**B**) lamina defect with visible spinal dural, and (**C**) electrospun fibrous membranes were laid on the lamina defect.

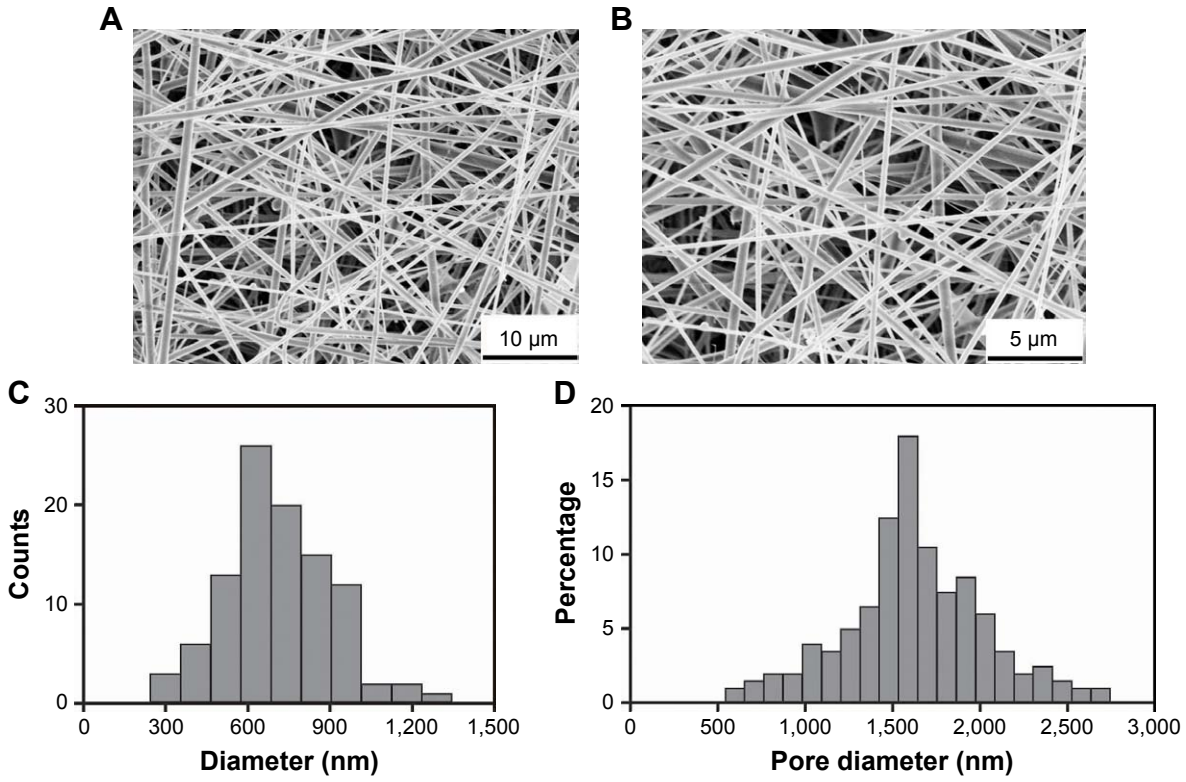

Figure 2 SEM micrographs of electrospun membranes with different magnifications (**A** and **B**); diameter and pore size distribution in ICA-loaded PCL–gelatin electrospun membranes (**C** and **D**).
Abbreviations: ICA, icariin; PCL, polycaprolactone; SEM, scanning electron microscopy.

no apparent beads and displaying a homogeneous distribution. The diameter of the microfibers ranged from 300 nm to 1,300 nm with the mean diameter of 760.69 nm±19.15 nm, which increased slightly with increasing ICA concentration (Figure 2C). The pore size distribution shifted from 0.6 μm to 2.7 μm with porosities of ~75%–86% for nutrient exchanges, which were deemed valid to prevent the penetration of fibroblasts through the membranes (Figure 2D).

Chemical, thermal and mechanical properties

According to the previous study, PCL-related stretching modes are represented by peaks at 2,866 cm^{-1} (symmetric CH_2 stretching), 1,721 cm^{-1} (C=O stretching) and 1,294 cm^{-1} (C–O and C–C stretching), and the characteristic peaks of gelatin appear at ~1,650 cm^{-1} (amide I).[19] As shown in Figure 3A, PCL–gelatin membranes appeared to show similar characteristic peaks corresponding to both PCL and gelatin. The ICA-related peaks appear between 1,604 cm^{-1} and 1,660 cm^{-1} (C=O and C=C stretching), and these peaks do not obviously change with increasing ICA content. However, the hydrogen bond interactions among PCL, gelatin and ICA caused light shift of the original absorption bands.

The DSC thermograms of the PCL–gelatin membranes demonstrated that melting peaks of the samples were observed at ~60°C (Figure 3B). Although the ICA contents were diverse in different membranes, the lack of other melting peaks showed that the ICA was uniformly dispersed at a molecular level.

To elucidate the mechanical properties of the PCL–gelatin membranes, the tensile strength was measured, and the stress–strain curves are shown in Figure 3C. Compared with control groups, there was a decrease in the maximum tensile strength on the ICA-loaded microfiber membranes, yet there was no significant difference between the PCL–gelatin and the ICA-loaded PCL–gelatin membranes. When the concentration of ICA was increased, we observed that the maximum tensile strength slightly decreased in the stress–strain curves.

The hydrophilicity of membranes has great influence on the adhesion of fibroblast cells. The electrospun ICA-loaded PCL/gelatin membranes are moderately hydrophobic with contact angles ranging from 126.4 to 97.3. As shown in Figure 3D, the incorporation of ICA content significantly changes the hydrophilicity of the membranes. With the increase in ICA content, the contact angle decreases because of the hydrophobicity of the ICA molecule.

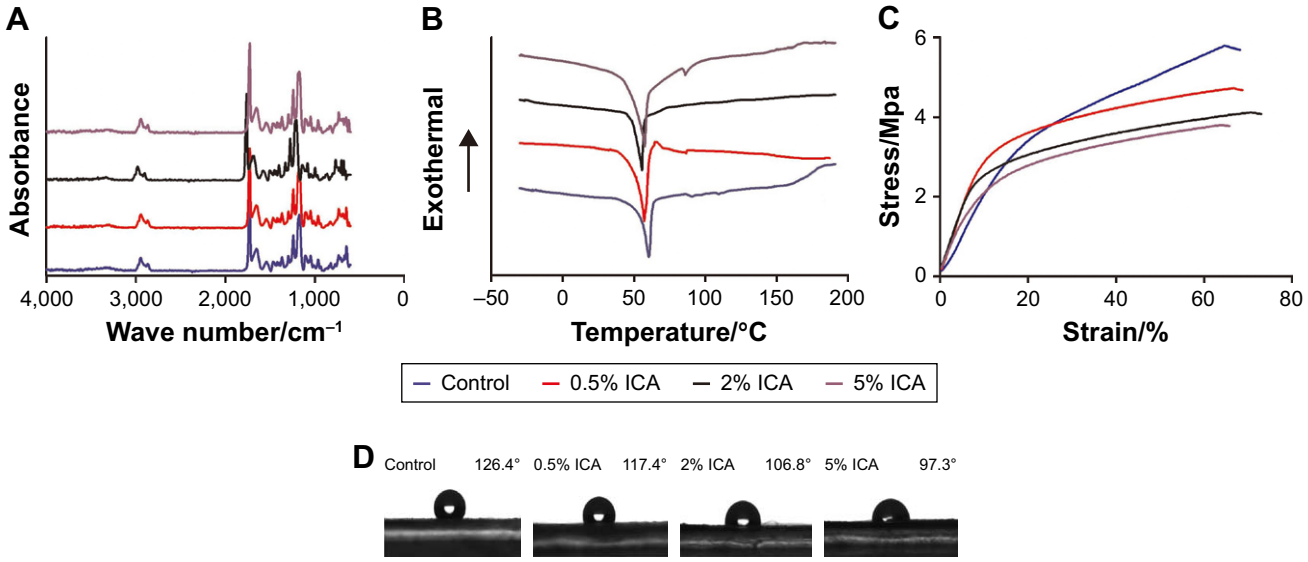

Figure 3 Chemical, thermal and mechanical properties of the ICA-loaded PCL–gelatin membranes: (**A**) FTIR spectra, (**B**) DSC thermograms, (**C**) stress–strain curves and (**D**) water contact angle.
Abbreviations: DSC, differential scanning calorimetry; ICA, icariin; PCL, polycaprolactone.

Drug release profile

The daily and cumulative release of ICA from the PCL–gelatin membranes is shown in Figure 4A and B. The ICA-loaded membranes had a burst release during the first 2 days and a slower release over 18 days. The loading efficiencies of ICA in 0.5 wt%, 2 wt% and 5 wt% PCL–gelatin membranes were 94.6%, 82.8% and 77.1%, respectively, which clearly shows that the cumulative percentage of ICA in the membranes at low concentrations is much higher than that in membranes loaded with high ICA content. On account of these diffusion characteristics, increasing the amount of ICA loaded onto the membranes resulted in an increase in the amount of ICA release, while the initial burst release was more distinct. The burst release stage is exactly when the inflammatory reaction happened, and the sustained release in the first week is capable of suppressing fibroblast migration and proliferation.

In vitro cell studies

Barrier function to fibroblast cells

The barrier function of the ICA-loaded PCL–gelatin electrospun membrane was determined in vitro by using the Cell Crown to conduct penetrant testing. The results showed that the fibroblast cells had favorable growing status on the frontal membrane, while no cells arrived at the opposite side of the membranes or adhered on the bottom of the culture dish due to the pore sizes being much smaller than the cell sizes (Figure 5A–C). This phenomenon demonstrated that

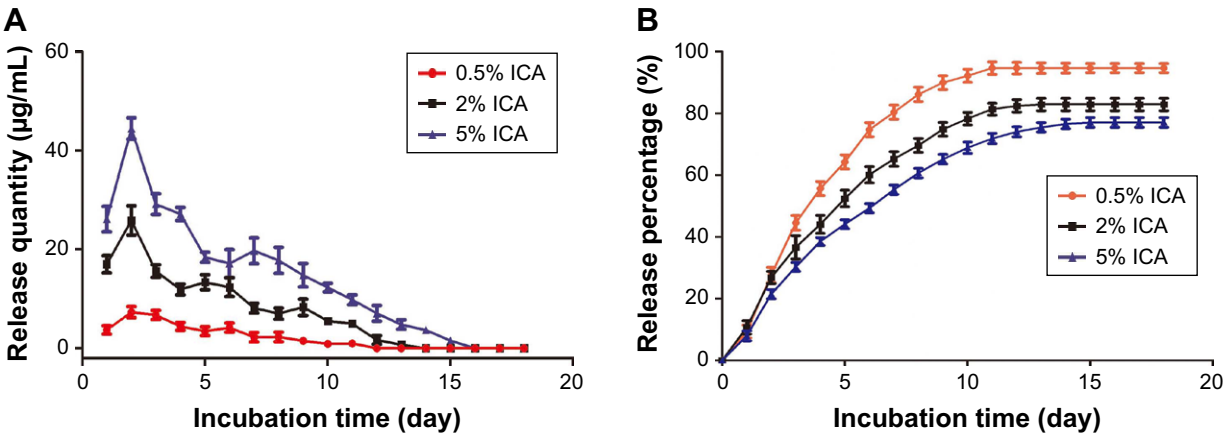

Figure 4 Daily (**A**) and cumulative (**B**) release of ICA from PCL–gelatin electrospun membranes after incubation in PBS at 37°C.
Abbreviations: ICA, icariin; PCL, polycaprolactone.

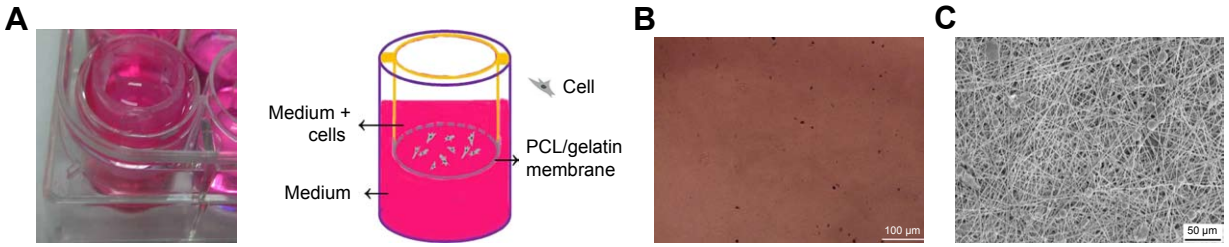

Figure 5 (**A**) The photographs and the schematic diagram on barrier function of ICA-loaded PCL/gelatin membranes. (**B**) The bottom of the 24-well plate after seeding cells on the membranes for 7 days. (**C**) SEM micrograph of the opposite side of the cell-cultured membrane for 7 days.
Abbreviations: ICA, icariin; PCL, polycaprolactone; SEM, scanning electron microscopy.

the membrane possesses good fibroblast cell barrier functionality after 7 days.

Cell cytotoxicity of ICA-loaded membrane

After sustained culture for 3 days, the viability of the fibroblast cells on different electrospun membranes was investigated using an MTT assay (Figure 6A). As shown in Figure 6B, the status of dead (orange)/live (green) cells on different extract solutions after 4 days of culture was analyzed. We observed that the number of dead cells increased as the ICA concentration increased, and therefore it is clear that the extract solution of ICA-loaded membranes significantly suppressed the viability of fibroblast cells. According to the RGR standard (RGR/%$<$50%), the observed cytotoxicity is still in an acceptable range even when the ICA concentration is $<$5%.

Cell adhesion and proliferation on membranes

Cell adhesion can influence the capacity of cell proliferation on the electrospun membrane, and this plays an important role in preventing tissue adhesion. After 1 day, 4 days and 7 days of culture, the proliferation of fibroblast cells on the surface of ICA-loaded membranes was compared by detecting the OD (Figure 7A). For all the detected membranes, the OD value of cell proliferation increased continuously during the 7 days of culture and showed significant differences between the control membrane and the 2 wt% and 5 wt% ICA-loaded membranes ($P<0.05$). The morphology of fibroblast cells proliferating on the PCL–gelatin membranes was observed by SEM and fluorescence microscopy after 4 days of seeding (Figure 7B and C). We observed that the number of cells with spindle morphology and larger cytoplasm was much greater in the control group, whereas the number of cells adhered onto the surface of the mat decreased as the ICA concentration increased. This result indicates that the cells forming adhesions were dramatically reduced and the membrane exhibited clear anti-adhesion effects.

In vivo animal study

In vivo degradation of electrospun membranes

The degradation rate of the PCL–gelatin membranes directly influences the integrity of the membrane, which in turn

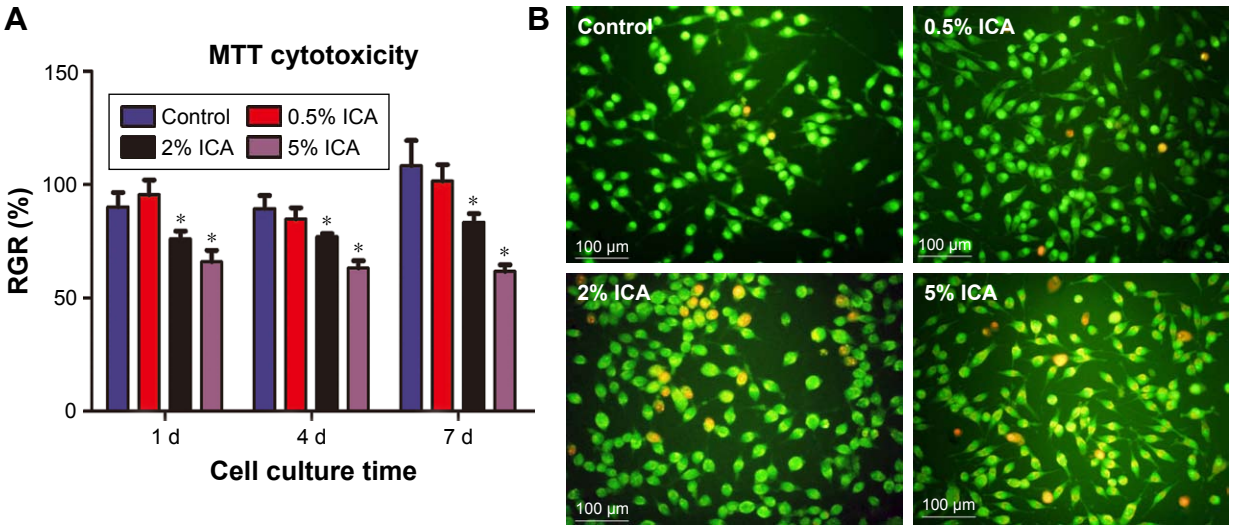

Figure 6 The RGR/% of fibroblast cells cultured in extract solutions of electrospun membranes (**A**) and dead/live cells staining for 4-day culture (*$P<0.05$ compared with the control group) (**B**) by using the AO-EB kit.
Abbreviations: AO-EB, acridine orange–ethidium bromide; d, day; ICA, icariin; RGR, relative growth rate.

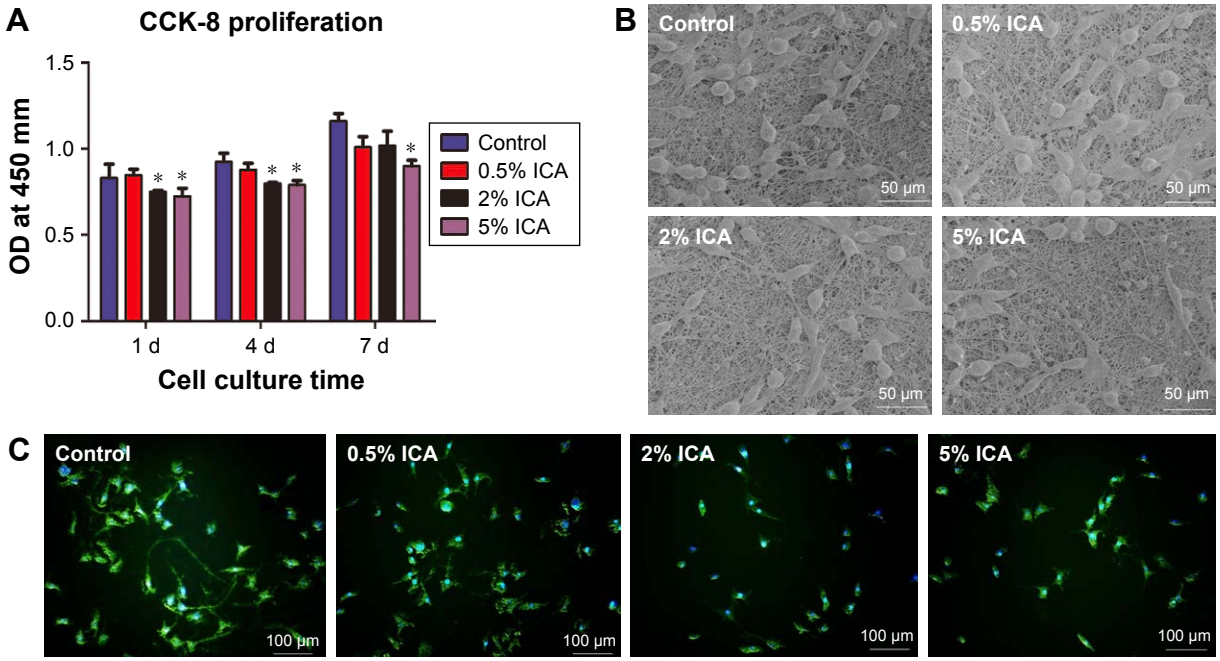

Figure 7 Cell adhesion and proliferation on the surface of different membranes.
Notes: (**A**) OD of fibroblast cells after 1 day, 4 days and 7 days (*$P<0.05$ compared with the control group); the SEM micrographs (**B**) and fluorescent images (**C**) of cells cultured for 4 days.
Abbreviations: CCK-8, Cell Counting Kit-8; d, days; ICA, icariin; SEM, scanning electron microscopy.

impacts on its ability to act as a barrier and therefore its overall anti-adhesion function. The morphological changes in the implanted membranes were observed by general observation and SEM after 4 weeks, 8 weeks and 12 weeks of implantation (Figure 8). The graphs showed that the ICA-loaded PCL–gelatin membranes retained the unique microfiber morphology with no obvious degradation during the preliminary 4 weeks; however, after 8 weeks we began to observe that the margins of membranes were absorbed, and some of the microfibers were broken. Dramatically after 12 weeks, we observed accelerated degradation, resulting in the appearance of large pores in the material.

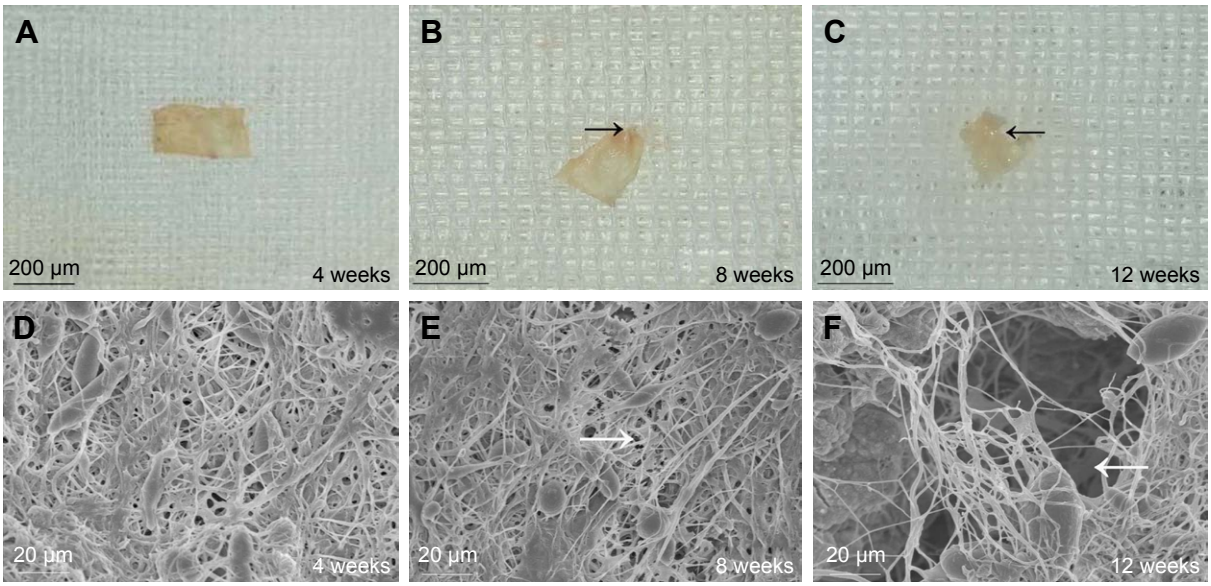

Figure 8 The morphology of the ICA-loaded PCL–gelatin membrane (**A**–**C**), and SEM micrographs of membrane surfaces (**D**–**F**) at different observation times after implantation.
Note: The black arrows indicate the absorbed margin, and the white arrows indicate the pores.
Abbreviations: ICA, icariin; PCL, polycaprolactone; SEM, scanning electron microscopy.

Adhesion scores and hydroxyproline content evaluation

After 4 weeks of implantation, the tissue adhesions were directly observed in the defect sites and were graded by the Rydell scores. The degree of adhesion in both the control and unloaded groups was dramatically worse than that observed in the ICA-loaded groups. Importantly, we also noted a decrease in the grade of severity of tissue adhesions with increasing ICA content, with 5 wt% ICA showing the lowest grades (Figure 9A). It has been reported that hydroxyproline is an important component of fibrous collagen and that it is proportional to the severity of scar formation.[20] From the quantified results obtained, we observed that the untreated group had the highest hydroxyproline concentration compared with that of the ICA-treated groups and showed that the tendency for scar formation decreased with increasing ICA content ($P<0.05$) (Figure 9B).

In vivo histological assessments

Four weeks after surgery, the adhesion tissues were obtained and evaluated by H&E and Masson staining, which provides a clear pictorial representation of the anti-adhesion effects of the membranes being tested in this study. H&E staining (Figure 10A) shows that adhesion tissues treated with ICA-loaded membranes are, on average, less than those with the unloaded group, in which dense population of adhesions formed. Additionally, we observed chronic inflammation around the spinal dural. Interestingly, few adhesion formations were observed in the ICA-loaded membrane groups, and the levels of formation of adhesion tissues slightly decreased as the ICA content increased. Meanwhile, Masson staining showed similar results, with defect sites filled with fibrous tissue in the unloaded group, while the ICA-loaded group exhibited excellent prevention toward adhesion formation (Figure 10B).

Protein expression in adhesion formations

To evaluate the cause of the anti-adhesive activity and explore the molecular mechanism for preventing tissue adhesion in the ICA-loaded PCL–gelatin membranes, the expression of col I, col III, α-SMA, TGF-β, Smad2 and Smad3 in adhesive fibrous tissue was determined by Western blotting (Figure 11). The results showed that col I and III proteins, which are the important components of adhesion tissues, were dramatically higher in the control and unloaded groups than those observed for the ICA-loaded membrane groups (Figure 11A). The α-SMA protein was also effectively suppressed in the ICA-loaded membrane groups. As shown in Figure 11B, the control group and unloaded membrane groups did not show significant differences in TGF-β and Smad2/3 expression, but the expression was clearly lower in the ICA-containing groups. The expression trends of col I/III, TGF-β and Smad2/3 protein levels were consistent in different groups, which indicated that ICA inhibited col I/III expression by downregulating the TGF-β-Smad2/3 signaling pathways.

Discussion

This study aimed to fabricate an anti-adhesion microfiber membrane, which was loaded or doped with ICA. The ICA within the structure was designed to be released in a controlled manner, and we aimed to investigate the anti-adhesion ability of ICA after laminectomy and subsequently study its mechanism of action. In this study, different concentrations (0.5 wt%, 2 wt% and 5 wt%) of ICA were incorporated into the PCL/gelatin electrospun microfibers, and the propensity of the ICA-loaded membranes to act as barriers was determined by in vitro and in vivo studies. The results showed that electrospun membranes were effective drug delivery carriers to achieve sustained release properties and inhibit adhesion formation successfully. Meanwhile, the ICA-loading

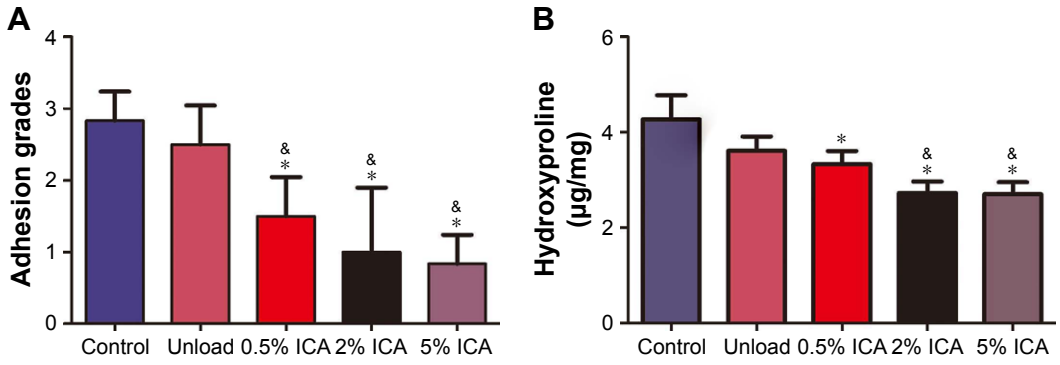

Figure 9 Gross evaluation of the adhesion formation (**A**) and hydroxyproline assessment (**B**) in untreated control, unloaded and ICA-loaded membrane groups.
Notes: $^{\&}P<0.05$ compared with the unloaded membrane group; $^{*}P<0.05$ compared with the control group.
Abbreviation: ICA, icariin.

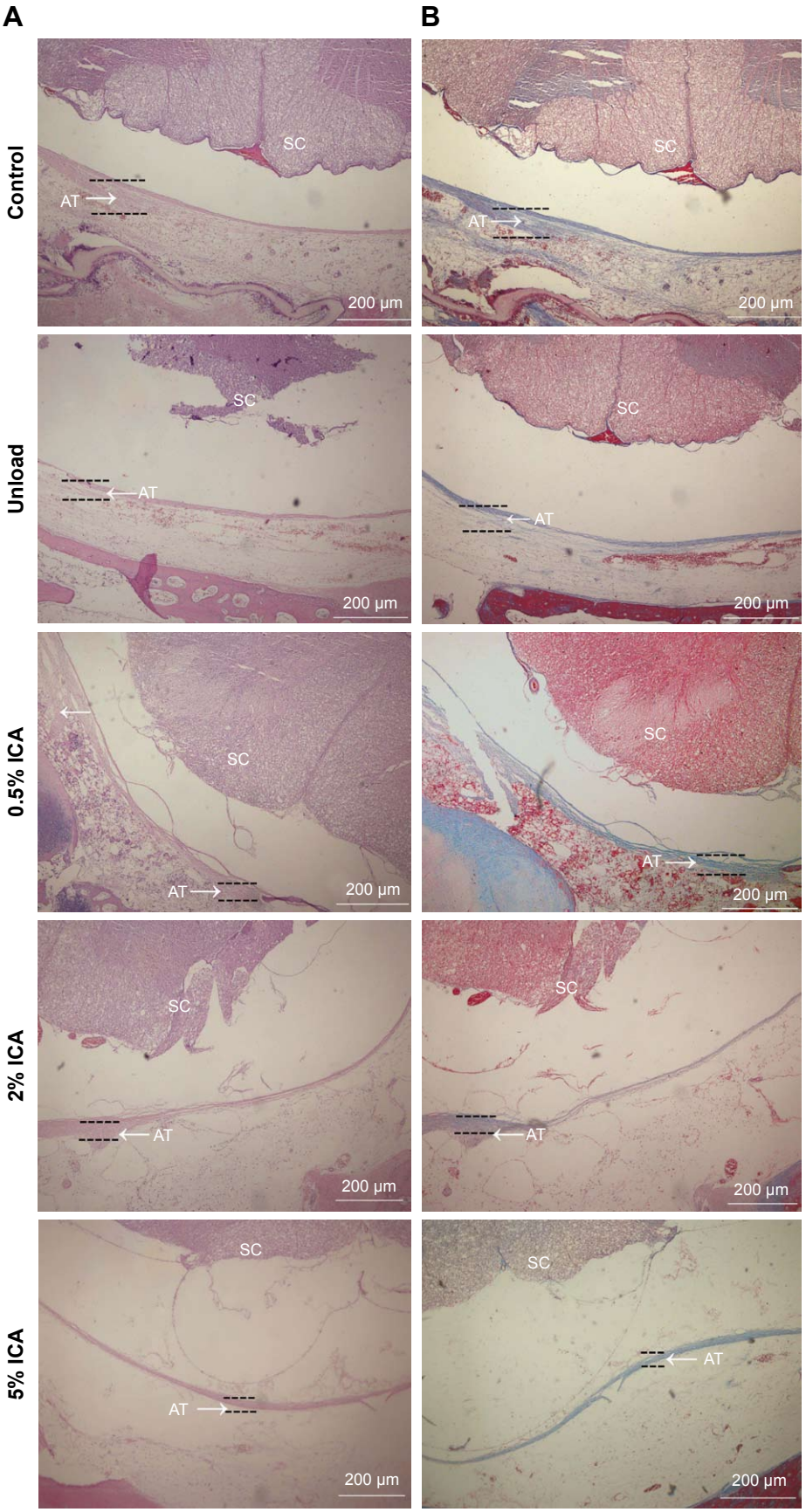

Figure 10 Histological micrographs of different PCL–gelatin membrane groups with H&E (**A**) and Masson (**B**) staining after laminectomy for 4 weeks.
Notes: Scale bar =200 μm. Arrows indicate the adhesion tissue.
Abbreviations: AT, adhesion tissue; ICA, icariin; PCL, polycaprolactone; SC, spinal cord.

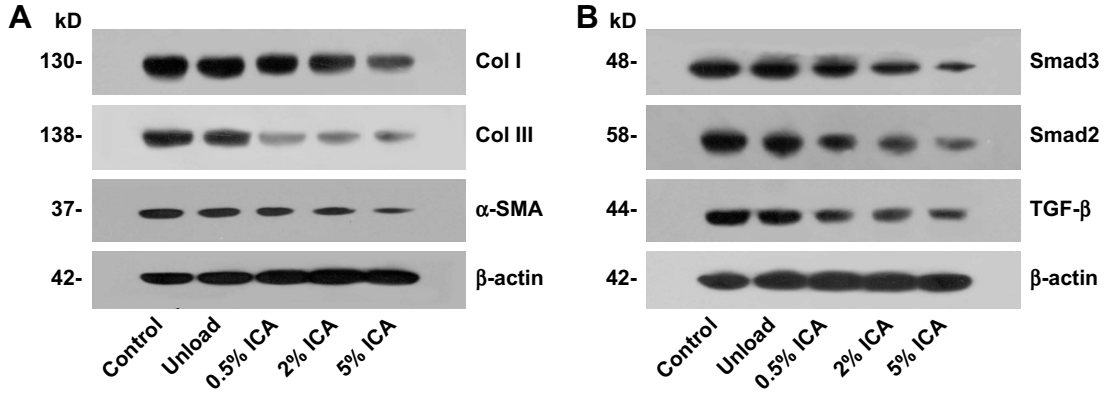

Figure 11 Western blot assay for col I/III, α-SMA (**A**) and TGF-β, Smad2/3 (**B**) expression in adhesion tissues with different membrane groups for 4 weeks.
Abbreviations: Col I, collagen I; Col III, collagen III; ICA, icariin; kD, k Daleon.

microfiber membranes were shown to have good biocompatibility and no clear toxicological issues from the in vitro and in vivo investigation.

The blending of natural gelatin and synthetic PCL for the delivery of bioactive molecules has many merits, such as increased biocompatibility, no observed immunogenicity and biodegradability with relatively tunable mechanical properties.[21,22] In the work previously carried out in our laboratory, we had solved the phase separation issues observed upon mixing PCL and gelatin through the addition of a small quantity of acetic acid into the electrospun solutions. This allowed the ICA to disperse homogeneously throughout the polymer matrix and thus extended the drug release time observed.[9] Other studies have demonstrated that the PCL/gelatin ratio used influences the mechanical properties, and low concentration gelatin (~30%) was sufficient to satisfy the required mechanical traits for biological application.[23,24] In this study, we utilized previous findings from our laboratory in relation to the optimum PCL/gelatin ratio and chose a mixture ratio of 80% PCL and 20% gelatin. We found that this ratio provides a membrane with enough mechanical strength, favorable drug encapsulation efficiencies and biodegradation rates to be used as an anti-adhesion membrane after successful laminectomies.

Electrospinning, as a means of fabrication, has attracted much attention in the field of drug delivery for uniform drug distribution and controlled drug release characteristics.[25] The PCL–gelatin membranes loaded with different concentrations of ICA exhibited lower burst release relative to other polymer/small molecule drug blending composite microfiber mats,[25,26] which was then followed by a long-term sustained release lasting for ~18 days. The mechanism of prolonged ICA release is based on homogeneous ICA microcrystal distribution inside the microfibers and the hydrogen bond interactions between the PCL/gelatin polymer and the microcrystal. The hydrogen bond interactions potentially slow down the initial burst release, while the inner microcrystal provides a more sustained slow release profile which can be correlated with the microfiber degradation rate. In comparison to conventional polymer/small molecule drug blending microfibers, whose release rate is in the order of several hours to days, the electrospun ICA membranes display a much-improved release profile.[26] Furthermore, the ICA is initially released from the membrane by diffusion from the membrane surface and is subsequently released through small pores in the dissolution medium, which means that the release rate can also be affected by the thickness of the membrane being used.[27,28] Although traditionally burst release is regarded as a negative phenomenon, it is typically within the first week post-operative that physicians note a high-incidence rate of inflammation and adhesion formation.[29] Therefore, an initial burst release within the first few days after a laminectomy is helpful in preventing detrimental inflammatory response as well as inhibiting the invasion of fibroblast cells before they begin to proliferate. As the concentration of ICA is increased both in vitro and in vivo, we found that the viability of fibroblasts gradually decreased and tissue adhesion was simultaneously prevented; however, 2% ICA and 5% ICA loading membrane groups showed no significant difference in adhesion formation. Therefore, considering the latent cytotoxicity and other potential side effects, the 2% ICA-loaded membrane was most suitable to be clinically applied as an anti-adhesion membrane.

Additionally, the electrospun ICA membranes can also act as a physical barrier and therefore partly block invasion of extrinsic fibroblast cells in adhesion progression, with this phenomenon being observed in in vivo experiments. The in vitro results revealed that fibroblast cells were capable of adhering onto PCL–gelatin membranes but could not penetrate

the fibrous membranes due to the smaller pore compared with cell size. Thus, the well-designed ICA-loaded membranes showed superior dual capacity acting as both a physical barrier and as a pharmacological agent to effectively prevent the process of adhesion formation. However, if this strategy is to be considered for future use in a clinical setting, these ICA-loaded membranes should be further studied to thoroughly investigate their anti-adhesion mechanism of action.

ICA has been reported to show tremendous pharmacological potential including its use as an anti-cancer agent, anti-inflammatory agent and anti-fibrosis treatment in different types of tissues.[4–6] However, the specific functions and mechanisms of ICA in anti-adhesion and collagen synthesis inhibition are still unexplored. Previous studies have demonstrated that TGF-β induces tendon adhesion formation by stimulating cell proliferation and collagen expression during tissue repair.[30–32] Further studies have shown that downregulation of Smad2/3 reduced col I/III synthesis and subsequently decreased tendon adhesion in tendon repair.[13,32] As is well known, TGF-β and Smad are constituent proteins in classical signaling pathways, which play crucial roles in suppression of cell proliferation and collagen expression. Therefore, we hypothesized that the ICA mechanism of action relies upon the regulation of the TGF-β/Smad2/3 pathway in fibroblast proliferation and col I/III expression to inhibit the process of adhesion. Our results showed that cell proliferation was negatively affected and col I/III syntheses were significantly decreased in the ICA-loaded membrane groups. The TGF-β and Smad2/3 expression was also downregulated at the same time. The changes in protein expression revealed that TGF-β is the target protein of ICA and works to directly block downstream Smad2/3, which in turn significantly reduces col I/III expression. In addition, adhesion-associated α-SMA was effectively suppressed in the ICA-loaded groups, which was not regulated by TGF-β but could account for the observed fibroblast apoptosis.[33] Therefore, we reason that ICA, as a potential anti-adhesion drug, might prevent tissue adhesion formation through diverse cellular signal transmissions, with regulation of TGF-β, Smad2/3 and col I/III levels playing a dominant role in this anti-adhesion treatment.

Conclusion

In this study, we have described a novel and efficient anti-adhesion ICA-loaded PCL–gelatin electrospun membrane after laminectomy, which can release ICA in a controlled and sustained manner. The ICA-loaded membranes have been shown to inhibit fibroblast proliferation and reduce collagen synthesis during adhesion formation in vivo through regulation of the TGF-β and Smad pathways. These results show that the ICA-loaded membranes can prevent adhesion formation effectively through both pharmacological and physical processes. We also describe the regulation mechanism of the ICA in tissue adhesions for the first time. Therefore, we believe that these ICA-loaded PCL/gelatin electrospun membranes show great potential in a clinical setting as anti-adhesion nanomaterials for postoperative repair. Finally, further clinical trials relating to ICA-loaded membrane's biosecurity are essential for future clinical application.

Acknowledgment

This work was supported by the National Natural Science Foundation of China (51673029, 81330043 and 81071499) and Beijing Talent Fund (2016000021223ZK34).

Disclosure

All the authors declare that they have no competing interests for any commercial associations and have no financial interests held by the author's family.

References

1. Daniell JR, Osti OL. Failed back surgery syndrome: a review article. *Asian Spine J*. 2018;12(2):372–379.
2. Gambardella G, Gervasio O, Zaccone C, Puglisi E. Prevention of recurrent radicular pain after lumbar disc surgery: a prospective study. *Acta Neurochir Suppl*. 2005;92:151–154.
3. Touliatos AS, Soucacos PN, Beris AE. Post-discectomy perineural fibrosis: comparison of conventional versus microsurgical techniques. *Microsurgery*. 1992;13(4):192–194.
4. Li C, Li Q, Mei Q, Lu T. Pharmacological effects and pharmacokinetic properties of icariin, the major bioactive component in Herba Epimedii. *Life Sci*. 2015;126:57–68.
5. Li YC, Ding XS, Li HM, Zhang C. Icariin attenuates high glucose-induced type IV collagen and fibronectin accumulation in glomerular mesangial cells by inhibiting transforming growth factor-β production and signalling through G protein-coupled oestrogen receptor 1. *Clin Exp Pharmacol Physiol*. 2013;40(9):635–643.
6. Kong L, Liu J, Wang J, et al. Icariin inhibits TNF-α/IFN-γ induced inflammatory response via inhibition of the substance P and p38-MAPK signaling pathway in human keratinocytes. *Int Immunopharmacol*. 2015;29(2):401–407.
7. Hu Y, Liu K, Yan M, Zhang Y, Wang Y, Ren L. Icariin inhibits oxidized low-density lipoprotein-induced proliferation of vascular smooth muscle cells by suppressing activation of extracellular signal-regulated kinase 1/2 and expression of proliferating cell nuclear antigen. *Mol Med* Rep. 2016;13(3):2899–2903.
8. Zeng J, Xu X, Chen X, et al. Biodegradable electrospun fibers for drug delivery. *J Control Release*. 2003;92(3):227–231.
9. Shi R, Xue J, Wang H, et al. Fabrication and evaluation of a homogeneous electrospun PCL–gelatin hybrid membrane as an anti-adhesion barrier for craniectomy. *J Mater Chem B*. 2015;3(19):4063–4073.
10. Chen SH, Chen CH, Fong YT, Chen JP. Prevention of peritendinous adhesions with electrospun chitosan-grafted polycaprolactone nanofibrous membranes. *Acta Biomater*. 2014;10(12):4971–4982.
11. Wang X, Ding B, Li B. Biomimetic electrospun nanofibrous structures for tissue engineering. *Mater Today*. 2013;16(6):229–241.

12. Sancak E, Erdem R. Functionalization techniques for electrospun nanofibers for drug delivery applications: a review. *Usak University Journal of Material Sciences*. 2014;3(2):180–180.
13. Jiang S, Zhao X, Chen S, et al. Down-regulating ERK1/2 and SMAD2/3 phosphorylation by physical barrier of celecoxib-loaded electrospun fibrous membranes prevents tendon adhesions. *Biomaterials*. 2014;35(37):9920–9929.
14. Lo HY, Kuo HT, Huang YY. Application of polycaprolactone as an anti-adhesion biomaterial film. *Artif Organs*. 2010;34(8):648–653.
15. Binulal NS, Natarajan A, Menon D, Bhaskaran VK, Mony U, Nair SV. PCL-gelatin composite nanofibers electrospun using diluted acetic acid-ethyl acetate solvent system for stem cell-based bone tissue engineering. *J Biomater Sci Polym Ed*. 2014;25(4):325–340.
16. Zhao Q, Wang S, Xie Y, et al. A rapid screening method for wound dressing by cell-on-a-chip device. *Adv Healthc Mater*. 2012;1(5):560–566.
17. Xue J, He M, Liu H, et al. Drug loaded homogeneous electrospun PCL/gelatin hybrid nanofiber structures for anti-infective tissue regeneration membranes. *Biomaterials*. 2014;35(34):9395–9405.
18. Rydell N, Balazs EA. Effect of intra-articular injection of hyaluronic acid on the clinical symptoms of osteoarthritis and on granulation tissue formation. *Clin Orthop Relat Res*. 1971;80(3):25–32.
19. Kim MS, Jun I, Shin YM, Jang W, Kim SI, Shin H. The development of genipin-crosslinked poly(caprolactone) (PCL)/gelatin nanofibers for tissue engineering applications. *Macromol Biosci*. 2010;10(1):91–100.
20. Sun Y, Yan LQ, Liang Y, Xl L, Cao XJ, Lu C. Reduction of epidural scar adhesion by topical application of simvastatin after laminectomy in rats. *Eur Rev Med Pharmacol Sci*. 2015;19(1):3–8.
21. Chong EJ, Phan TT, Lim IJ, et al. Evaluation of electrospun PCL/gelatin nanofibrous scaffold for wound healing and layered dermal reconstitution. *Acta Biomater*. 2007;3(3):321–330.
22. Lim YC, Johnson J, Fei Z, et al. Micropatterning and characterization of electrospun poly(ε-caprolactone)/gelatin nanofiber tissue scaffolds by femtosecond laser ablation for tissue engineering applications. *Biotechnol Bioeng*. 2011;108(1):116–126.
23. Jiang YC, Jiang L, Huang A, Wang XF, Li Q, Turng LS. Electrospun polycaprolactone/gelatin composites with enhanced cell-matrix interactions as blood vessel endothelial layer scaffolds. *Mater Sci Eng C Mater Biol Appl*. 2017;71:901–908.
24. Strobel HA, Calamari EL, Beliveau A, Jain A, Rolle MW. Fabrication and characterization of electrospun polycaprolactone and gelatin composite cuffs for tissue engineered blood vessels. *J Biomed Mater Res B Appl Biomater*. 2018;106(2):817–826.
25. Lu Y, Huang J, Yu G, et al. Coaxial electrospun fibers: applications in drug delivery and tissue engineering. *Wiley Interdiscip Rev Nanomed Nanobiotechnol*. 2016;8(5):654–677.
26. Xue J, Niu Y, Gong M, et al. Electrospun microfiber membranes embedded with drug-loaded clay nanotubes for sustained antimicrobial protection. *ACS Nano*. 2015;9(2):1600–1612.
27. Liu Q, Zhang ZR, Yin LH, Cheng WX, Qin ZS. Materials research of SF/COL/PLCL and SF/COL/PLLA electrospun three-dimensional nanofiber scaffold. *J Funct Mater*. 2014;45(3):3141–3144.
28. Bigi A, Cojazzi G, Panzavolta S, Rubini K, Roveri N. Mechanical and thermal properties of gelatin films at different degrees of glutaraldehyde crosslinking. *Biomaterials*. 2001;22(8):763–768.
29. Tatsui CE, Martinez G, Li X, Pattany P, Levi AD. Evaluation of DuraGen in preventing peridural fibrosis in rabbits. Invited submission from the Joint Section Meeting on Disorders of the Spine and Peripheral Nerves, March 2005. *J Neurosurg Spine*. 2006;4(1):51–59.
30. Zhou Y, Zhang L, Zhao W, Wu Y, Zhu C, Yang Y. Nanoparticle-mediated delivery of TGF-β1 miRNA plasmid for preventing flexor tendon adhesion formation. *Biomaterials*. 2013;34(33):8269–8278.
31. Zhou MP, Yuan-Li HE, QL, et al. Expression and significance of TGF- β_1 and Smad2/3 in endometrium of women with intrauterine adhesions. *Guangdong Medical Journal*. 2014;35(12):1844–1847.
32. Katzel EB, Wolenski M, Loiselle AE, et al. Impact of Smad3 loss of function on scarring and adhesion formation during tendon healing. *J Orthop Res*. 2011;29(5):684–693.
33. Zhao X, Jiang S, Liu S, et al. Optimization of intrinsic and extrinsic tendon healing through controllable water-soluble mitomycin-C release from electrospun fibers by mediating adhesion-related gene expression. *Biomaterials*. 2015;61:61–74.